

EXCITATION OF MANTLE LOVE WAVES AND DEFINITION OF MANTLE WAVE MAGNITUDE

BY JAMES N. BRUNE AND GLADYS R. ENGEN

ABSTRACT

A study is made of the excitation of mantle Love waves of 100 seconds period as a function of magnitude. 153 measurements of Love wave spectral density for earthquakes since 1930 ranging in magnitude from 6.0 to 8.9 are used to determine an excitation curve. The observations were first corrected to a standard distance of 90° . The excitation curve supports earlier results for mantle Rayleigh waves and, for strike-slip motion, an earlier curve for seismic moment versus mantle-wave magnitude. For dip-slip motion, the moments should be multiplied by a factor of about $2\frac{1}{2}$. A definition of mantle wave magnitude M_M , is set up, and the largest earthquake since 1930 found on this scale is the Alaskan earthquake of March 28, 1964 where $M_M = 8.9$. Other comparably large earthquakes, $M_M = 8.8$, were the Kamchatka earthquake of November 4, 1952 and the Chilean earthquake of May 22, 1960. It is suggested that mantle-wave magnitudes be used as a diagnostic aid in estimating the Tsunami potential of earthquakes.

INTRODUCTION

In a previous paper the excitation of mantle Rayleigh waves of 100 seconds period as a function of magnitude was studied (Brune and King, 1967). We here study the excitation of mantle Love waves of 100 seconds period. It is important to study the excitation of long-period mantle waves because of the information they contain about source mechanism. The amplitudes of waves with period and wavelength long as compared to the time duration and dimensions of the source are directly proportional to the seismic moment of the equivalent double couple which, in turn, is proportional to the product of the rigidity, the area of the dislocation, and the average displacement over the dislocation surface (Maruyama, 1963). Long-period mantle waves are less affected by irregularities in the source mechanism, regional variations in earth structure and scattering and attenuation than shorter-period waves, and thus are simpler to interpret. Theoretical calculations for the excitation of mantle waves are available (Ben-Menahem and Harkrider, 1964).

Brune (1968) has recently used the technique of summing moments to calculate the seismic rate of slip along a given fault zone. He used the results of Brune and King (1967) to determine the shape of a seismic moment versus magnitude curve, and used geodetic and field observations of fault moment as given by Brune and Allen (1967) to set the absolute value of the curve. In this study a curve for the excitation of mantle Love waves as a function of magnitude is obtained from measurements of spectral density of Love waves at a period of 100 seconds. The results of this study support the previous results for excitation of mantle Rayleigh waves and for seismic moment versus magnitude.

Using the excitation curves for mantle Love and Rayleigh waves of 100 seconds period, a definition of mantle-wave magnitude is set up. This magnitude system has several advantages over those based on shorter period waves, but should be thought of as an independent determination of magnitude at a different portion of the spectrum and not an alternate definition of an absolute magnitude.

DATA

Seismograms used in this study were from a wide variety of instruments. For lower magnitudes, records from the ultra-long period seismographs described by Gilman (1960), and records from the WWNSS were used. For larger earthquakes Milne-Shaw, Wiechert, McComb-Romberg, Wenner, long-period Benioff and Benioff strain meter records were used. Table 1 describes these instruments. Although the magnifications of the older instruments are in some cases uncertain, the uncertainty is not large compared to the expected range of amplitudes and is probably not systematic. Amplitude spectral densities of mantle Love waves at a period of 100 seconds are the basic

TABLE 1
INSTRUMENTS

Stations	Instrument	Ampl. at 100 Sec
PAS	Gilman ULP NS	590
PAS	Gilman ULP EW	480
PAS	Gilman ULP EW	1960
PAS	Gilman ULP EW	290
ALQ, ANT, BOZ, CMC, NNA	WWNSS	430
COP, LAH, NOR, STU	WWNSS	108
DUG, MNN	WWNSS	1200
HNR	WWNSS	290
MAT, QUE, TRI	WWNSS	890
ATU, COL, MSH, NDI, NUR, RCD, SHI	WWNSS	210
OTT, SFA, TNT, VIC	Milne-Shaw	4
SJP	Wenner	9.4
BOZ, SLC	McComb-Romberg	3.2
CHI	McComb-Romberg	3.35
COL	McComb-Romberg	2.0
CSC, UKI	McComb-Romberg	1.07
TUC	Wood-Anderson	2.76
JEN, BER	Wiechert	1.5*
PAS	Strain	4.4*
PAS	Strain	4.0*
KIP	Strain	28*
PAS	L. P. Benioff	25*

* From Brune & King (1967).

data for this study. Spectral densities were determined by Fourier analysis both graphically and with the aid of a 7090 computer. Amplitude spectral densities rather than simple amplitudes were used since mantle Love waves are not sufficiently dispersed for the stationary phase approximation to be valid, i.e., the wave is pulse-like. This pulse-like wave has been named the G wave after Gutenberg by Byerly (1926). Typical G waves used in this study are shown in Figure 1. The amplitude spectral densities are corrected to a standard distance of 90°. The correction curve is given in Figure 2. This curve corresponds to the function $(\sin \Delta^\circ)^{1/2} \cdot e^{\pi(x-10000)/QU^T}$ where Δ is the distance in degrees, x is the distance in kilometers, U is the group velocity, T is the period, and Q is the seismic quality factor. Q is taken to have a value of 107 at $T = 100$ sec as found by Ben-Menahem (1965). The validity of the correction has been checked by numerous comparisons of reduced spectral densities from G1 and G3, G2 and G4, and G3 and G5 waves. Amplitude spectral densities determined for 153 recordings of mantle Love waves (corrected to a distance 90°) are given in Table 2, and the corresponding amplitude spectral densities averaged for each earthquake are

plotted as a function of magnitude in Figure 3. For earthquakes earlier than 1956 the magnitude values cited are those given in Richter (1958) when $M > 7.9$ and those given in Gutenberg and Richter (1954) when $M < 7.9$. For earthquakes after 1956 the magnitude cited is the magnitude assigned by Pasadena.

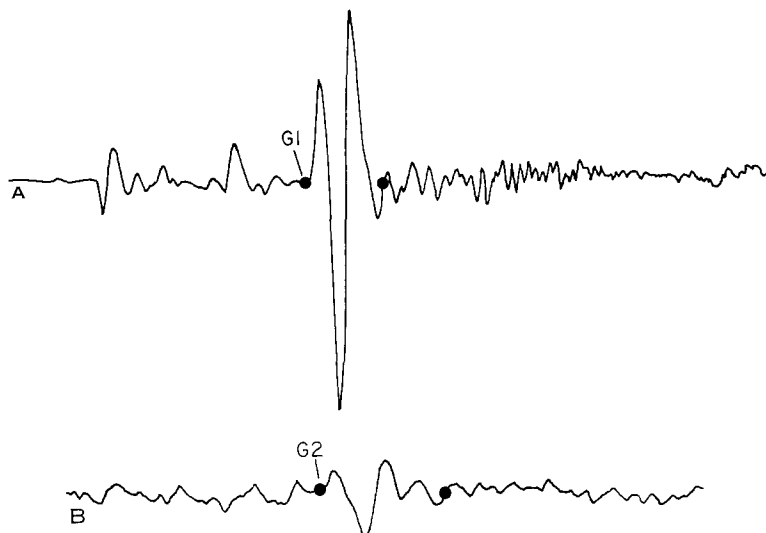


FIG. 1. Seismograms illustrating typical mantle Love waves used in this study. The seismogram illustrating G1 is for the Easter Island shock of 7 March 1963 ($M = 6\frac{3}{4}$); G2 is for the Kermadec Islands shock of 20 May 1963 ($M = 6\frac{1}{4}$ -7). Both were recorded on a CIT ULP instrument at Pasadena (Gilman, 1960).

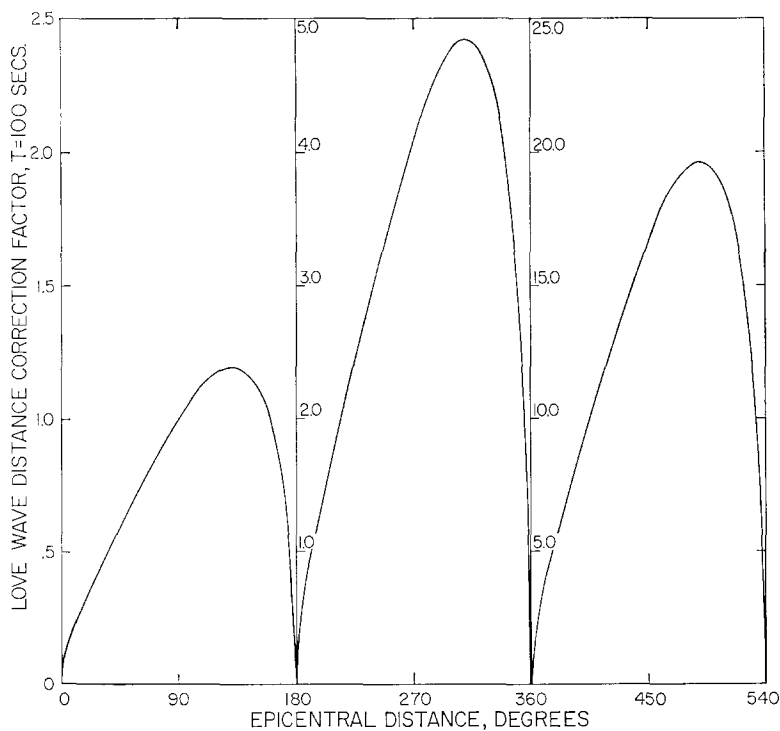


FIG. 2. Spectral density distance correction factor for 100 second period mantle Love waves. The correction curve may be extended to larger distances using the equation given in the text.

TABLE 2

Mag	Date	O.T.	Epicenter		Depth* (kms)	Sta.	Epic. Dist. (de- grees)	Phase	Sp. Dens. (cm-sec)	Log Sp. Dens.	Log Av. Sp. Dens.	
			lat	long								
6	5/27/67	172258.7	51.9N	176.1E	34	PAS	50	G1	.008050	-2.094	-2.094	
	3/23/66	000434.7	23.8N	122.8E	51	MSH	55	G1	.2502	-.602		
6-6½	5/19/66	070626.8	54.1N	164.1W	28	QUE	310	G2	.1094	-.961		
		020108.5	37.9N	13.1E	33	ANT	192	G2	.00323	-1.030	-.918	
	11/15/67	213151.5	28.7S	71.2W	15	LAH	43	G1	.04997	-1.301		
	6.2	1/21/68	164229.2	1.2S	14.0W	33	COL	68	G1	.1008	-.997	
							PAS	38	G1	.01759	-1.755	-1.755
					PAS	96	G1	.01964	-1.707	-1.707		
					PAS	77	G1	.1275	-.894	-.894		
					PAS	103	G1	.09846	-1.007	-1.020		
					PAS	258	G2	.09240	-1.034			
	6½	6/10/63	041638.4	55.3S	146.2E	33	PAS	121	G1	.01948	-1.710	-1.603
						PAS	240	G2	.03042	-1.517		
					PAS	99	G1	.01700	-1.770	-1.770		
					NDI	61	G1	.1574	-.803	-.846		
					NDI	299	G2	.1279	-.893			
					PAS	86	G1	.07716	-1.113	-1.113		
					PAS	108	G1	.4887	-.311	-.311		
					PAS	61	G1	.1244	-.905	-1.040		
					PAS	299	G2	.05792	-1.237			
					PAS	71	G1	.006478	-2.189	-2.189		
6½-6¾	3/31/63	053049.8	29.9S	177.9W	55	PAS	85	G1	.03216	-1.493	-1.493	
		063904.1	55.2S	146.1E	19	PAS	121	G1	.02056	-1.687	-1.494	
					PAS	240	G2	.04354	-1.361			
					PAS	116	G1	.04115	-1.386			
					PAS	244	G2	.02673	-1.573			
					CMC	83	G1	.1449	-.839	-.953		
					ALQ	116	G1	.1728	-.763			
					BOZ	105	G1	.1848	-.733			
					NOR	60	G1	.09855	-1.006			
					PAS	76	G1	.1143	-.942	-.942		
6.3-6.5	1/6/68	232721.7	27.8S	71.1W	33	PAS	77	G1	.02037	-1.691	-1.691	
	1/8/68	215420.8	14.8S	174.8W	16	PAS	77	G1	.02037	-1.691	-1.691	
	4/15/60	032538	27S	113W	0	PAS	61	G1	.02103	-1.677	-1.677	
6.5	1/1/63	233909.5	56.6N	157.5W	80	PAS	35	G1	.01524	-1.817	-1.817	
	3/6/66	021556.7	31.6N	80.5W	44	ATU	46	G1	.3041	-.517		
					ATU	314	G2	.3227	-.491			
					COP	52	G1	.04687	-1.329			
					COP	308	G2	.05019	-1.299	-.665		
					TRI	307	G2	.1635	-.786			
					STU	305	G2	.3707	-.431			
					LPA	145	G1	.2560	-.592			
					PAS	85	G1	.01066	-1.972	-1.972		
					PAS	129	G1	.2115	-.675	-.675		
					PAS	72	G1	.02878	-1.541	-1.628		
					PAS	72	G1	.01827	-1.738			
					PAS	37	G1	.03023	-1.520	-1.520		
					PAS	96	G1	.03933	-1.403	-1.403		
					PAS	233	G2	.09995	-1.000	-1.000		
6¾	3/29/60	063054	17S	167E	0	PAS	87	G1	.1141	-.943	-.764	
						PAS	273	G2	.2307	-.637		
					PAS	60	G1	.05535	-1.257	-1.257		
					PAS	90	G1	.0700	-1.155	-1.155		
					PAS	53	G1	.01111	-1.954	-1.954		
					PAS	99	G1	.1171	-.931	-.920		
					PAS	261	G2	.1235	-.908			
					RCD	105	G1	.3277	-.485			
					RCD	465	G3	.6284	-.202			
					RCD	255	G2	.3058	-.515	-.410		
					SHI	100	G1	.3045	-.516			
					NOR	104	G1	.4285	-.368			
					NNA	129	G1	.3378	-.471			

TABLE 2—Continued

Mag	Date	O.T.	Epicenter		Depth* (kms)	Sta.	Epic. Dist. (de- grees)	Phase	Sp. Dens. (cm sec)	Log Sp. Dens.	Log Av. Sp. Dens.
			lat	long							
	5/21/67	184511.7	1.0S	101.5E	173	PAS	131	G1	.02720	-1.565	-1.565
	10/4/67	172120.7	5.7S	153.9E	52	PAS	92	G1	.3010	-.521	-.521
	10/18/67	011145	79.8N	2.4E	33	PAS	62	G1	.2269	-.644	-.644
	1/19/68	060438.2	9.4S	158.4E	33	PAS	93	G1	.1936	-.713	-.746
						PAS	267	G2	.1649	-.783	
6½-7	3/26/63	004820.3	29.7S	177.9W	48	PAS	85	G1	.4321	-.364	-.370
						PAS	275	G2	.4208	-.376	
	5/20/63	113805.3	30.7S	178.3W	68	PAS	275	G2	.1041	-.983	-.983
	10/20/63	005307.2	44.7N	150.7E	25	PAS	292	G2	1.679	.225	.225
	5/20/65	004010.9	14.7S	167.4E	59	PAS	86	G1	.2036	-.691	-.831
						PAS	274	G2	.09180	-1.037	
	3/20/66	014249.9	0.6N	30.2E	36	PAS	135	G1	1.059	-.975	-.975
	3/4/67	175806.4	39.2N	24.6E	33	PAS	99	G1	.1965	-.707	-.707
7	6/20/60	020108	38S	73½W	0	PAS	277	G2	.6050	-.218	-.218
	11/24/60	065241.1	24.2S	176.1W	23	PAS	280	G2	.9070	-.045	-.045
	3/16/63	084451.1	46.6N	154.8E	46	PAS	296	G2	1.262	.101	.020
						PAS	65	G1	.8321	-.080	
	4/19/63	073522.7	35.7N	96.9E	33	PAS	464	G3	1.028	.012	-.180
						PAS	256	G2	.2942	-.532	
	12/21/67	022521.6	21.8S	70.0W	33	PAS	288	G2	2.945	.469	.469
	8/19/66	122209.6	39.2N	41.7E	26	PAS	105	G1	.08645	-1.438	-1.438
7-7½	8/2/65	131955.9	56.2S	158.2E	33	PAS	115	G1	.1667	-.778	
						HNR	313	G2	3.787	.575	.220
						MAT	454	G3	2.384	.377	
						NUR	156	G1	.3330	-.482	
	2/12/68	054447.6	5.5S	153.2E	74	PAS	268	G2	1.723	.236	.236
7½	5/21/60	100250	37½S	73½W	0	CHI	80	G1	4.612	.664	.664
7½-7½	5/22/60	103243	37½S	73W	0	SLC	86	G1	.1415	-.849	-.849
	11/1/60	084601.9	38.4S	74.4W	97	PAS	83	G1	.3252	-.488	-.392
						PAS	277	G2	.4854	-.314	
	9/15/63	004654.1	10.3S	165.6E	43	PAS	85	G1	.4985	-.302	-.302
7.4	4/1/46	122854	52½N	163½W		BOZ	34	G1	8.412	.925	
						BOZ	326	G2	4.646	.667	
						CHI	50	G1	3.897	.591	
						CHI	310	G2	3.799	.580	
						COL	346	G2	5.006	.699	
						COL	374	G3	7.637	.883	.844
						CSC	59	G1	8.511	.930	
						SLC	36	G1	4.421	.646	
						UKI	31	G1	5.241	.719	
						WES	418	G3	9.997	1.000	
						TUC	43	G1	15.18	1.181	
7.5	9/12/64	220658.5	49.05S	164.26E	33	DUG	475	G3	1.063	.027	
						DUG	605	G4	.5340	-.272	-.099
						MNN	489	G3	.7911	-.102	
7.7	7/18/34	013624	8N	82½W		VIC	53	G1	2.959	.471	.471
7.9	6/17/28	031927	16½N	98W		VIC	321	G2	12.04	1.081	1.081
	8/10/31	211840	47N	90E		SFA	277	G2	31.49	1.498	1.498
8.1	6/3/32	103650	19.5N	104.25W		VIC	327	G2	16.43	1.216	1.216
	7/18/34	194015	11½S	166½E		TNT	245	G2	5.447	.736	.736
8½-8½	5/22/60	191120	38S	73½W	0	SLC	274	G2	69.54	1.842	1.861
						CHI	280	G2	75.67	1.879	
8.3	9/1/23	025836	35½N	139½E		OTT	266	G2	20.62	1.314	1.314
	12/1/28	040610	35S	72W		VIC	265	G2	4.857	.686	.686
	5/14/32	131100	.5N	126.E		TNT	230	G2	5.722	.758	
						VIC	257	G2	5.877	.769	1.017
						SFA	231	G2	19.62	1.292	
	8/6/42	233659	14N	91W	50-60	COL	64	G1	2.133	.329	.383
						CHI	332	G2	2.694	.430	

TABLE 2—Continued

Mag	Date	O.T.	Epicenter		Depth* (kms)	Sta.	Epic. Dist. (de- grees)	Phase	Sp. Dens. (cm-sec)	Log Sp. Dens.	Log Av. Sp. Dens.
			lat	long							
8.4	2/3/23	160141	54N	161E	50-60	VIC	405	G3	65.67	1.817	1.822
						VIC	405	G3	66.95	1.826	
	1/15/34	084318	26½N	86½E		SJP	488	G3	8.312	.920	.920
						5/24/40	163357	10½S	77W	SJP	329
	11/4/52	165826	52.75N	159.5E		CHI	53	G1	4.290	.632	
						SFA	433	G3	48.51	1.686	
						OTT	290	G2	37.33	1.572	
						OTT	430	G3	69.59	1.843	
						SLC	304	G2	41.36	1.617	1.751
						CHI	293	G2	54.86	1.739	
						BOZ	305	G2	76.26	1.882	
						SJP	459	G3	49.49	1.695	
						SJP	621	G4	73.03	1.864	
						3/28/64	033610	61.1N	147.8W	33	SJP
8.6	2/1/38	190418	5½S	130½E	JEN	293	G2	97.94	1.991	1.876	
					JEN	653	G4	85.49	1.932		
					BOZ	113	G1	12.53	1.098		
					COL	451	G3	63.38	1.802	1.539	
8.6	8/24/42	225027	15S	76W	50-60	CHI	302	G2	5.796	.763	.675
					COL	96	G1	3.672	.565		
	3/4/52	012243	42½N	143E	SJP	474	G3	13.82	1.141		
					CHI	444	G3	28.32	1.452	1.242	
	SLC	72	G1	10.17	1.007						
	8.7	11/10/38	201843	55½N	158W	SJP	436	G3	18.06	1.257	1.167
						CHI	406	G3	11.31	1.053	
		6/26/41	115203	12½N	92½E	50-60	SLC	123	G1	1.215	.085
COL						91	G1	3.032	.482	.666	
COL	269	G2	9.668	.985							
8/15/50	140930	28½N	96½E	CHI	470	G3	59.80	1.777	1.777		
8.9	3/2/33	173054	39½N	144½E	BOZ	71	G1	7.341	.866	1.165	
					SJP	476	G3	21.90	1.340		

* Unless otherwise noted, depth is normal.

The data cover a magnitude range from 6.0 to 8.9 and a range of spectral densities from .0065 cm-sec to 97.94 cm-sec. The data are in good agreement with a curve having the shape of the X_{20}/X_{100} curve given by Brune and King for mantle Rayleigh waves. The deflection of this curve between magnitudes 7 and 7.1 is due to the interference effects of a propagating rupture. The curve has been fitted to the data by adjusting its level so that an equal number of observations fall above and below the curve. The scatter of the data from a single line is about one magnitude unit, i.e., a factor of 10. This is about the same scatter as observed for mantle Rayleigh waves.

SEISMIC MOMENT

A curve for seismic moment versus magnitude was derived from the shape of the 100 second mantle Rayleigh wave amplitude versus magnitude curve by Brune (1968). Using the theoretical curves of Ben-Menahem and Harkrider (1964) we also can set the moment versus magnitude scale for our data by finding the moment corresponding to spectral density of a given magnitude, e.g., $M = 6$. The spectral density for $M = 6$ taken from the curve in Figure 3 is .0229 cm-sec. For a pure strike-slip fault at a depth of 10 km observed at an average azimuth this corresponds to a seismic moment of 1.59×10^{25} dyne-cm. For a pure dip-slip motion on a fault dipping 60° this corresponds to a seismic moment of 3.89×10^{25} dyne-cm. An average for 100 cases of fault orientation and depth was found to be 3.09×10^{25} dyne-cm. In these cases dip was varied

from 10° to 90° , motion was varied from pure dip-slip to pure strike-slip and depth was varied from 10 km to 60 km. A value of Q equal to 107 was assumed, and a correction of 0.8 was used for sphericity.

On the basis of the above calculations we estimate that the mantle Love wave amplitude spectral density for $M = 6$, .0229 cm-sec., corresponds to a source moment of 1.66×10^{25} dyne-cm* for the case of pure strike-slip motion. This value is not significantly different from the value taken from the curve for moment versus magnitude obtained by Brune using observations of field displacement during faulting, and

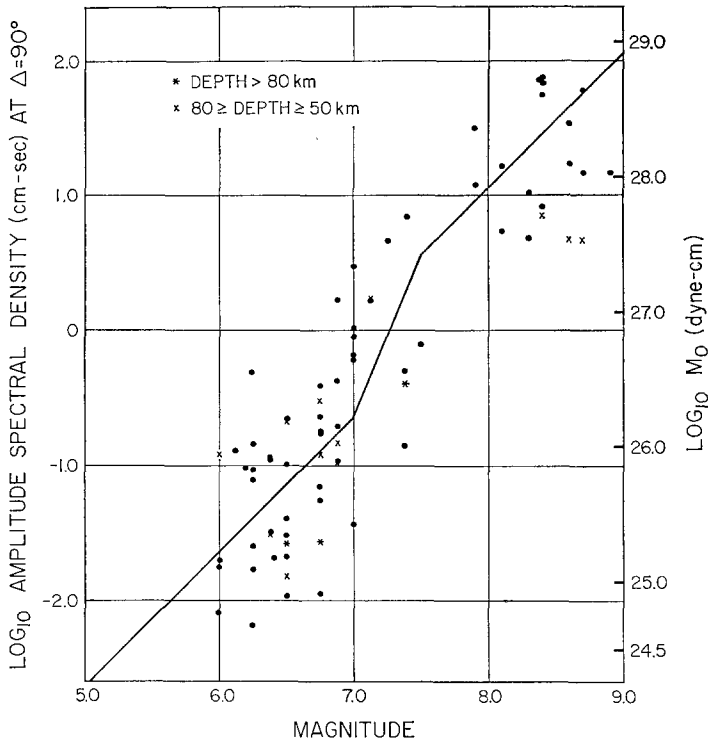


FIG. 3. Logarithm to the base 10 of mantle Love wave spectral densities averaged for each earthquake at a distance of 90° , plotted as a function of magnitude, M . The curve fitted to the points has the shape of the X_{20}/X_{100} curve of Brune and King (1967) for mantle Rayleigh waves and is used in the definition of mantle wave magnitude.

therefore the same scale on the right hand margin of Figure 3 is retained for strike-slip motion. For dip-slip motion, the moment obtained from this scale should be multiplied by a factor of about $2\frac{1}{2}$. When possible, the mantle wave magnitude, described below, rather than the 20 second surface-wave magnitude, should be used to estimate source moment.

DEFINITION OF MANTLE WAVE MAGNITUDE

Having curves for the excitation of both mantle Love waves and mantle Rayleigh waves as a function of magnitude, it is possible to define mantle wave magnitude M_M , by these curves. Mantle wave magnitude is determined independently using 100 second period Love waves and 100 second period Rayleigh waves, and the two values are averaged by averaging their antilogs. When data for more than one station are available, all values obtained are averaged ($M_M = \text{Log} [\text{average of antilogs of indi-}$

* Average for depths varying from 10-60 km.

vidual M_M 's]). This averaging will tend to remove scatter in the determination of magnitude, since it is unlikely that a given station will be at a node in the radiation pattern for both Love waves and Rayleigh waves. An example of such a calculation is given in Table 3. The curves defining magnitude are given in Figure 3 for Love waves

TABLE 3
EXAMPLE OF AVERAGING VALUES

Date	Earthquake	Sta.	Mantle Love Mag	Mantle Rayleigh Mag	Station Mag	Mantle Wave Mag
3/4/52	Japan	SJP	8.1	7.5	7.9	
		CHI	8.4	8.4	8.4	
		SLC	8.0	8.4	8.2	8.3

Mag = log (average of antilog of Love and Rayleigh mags).

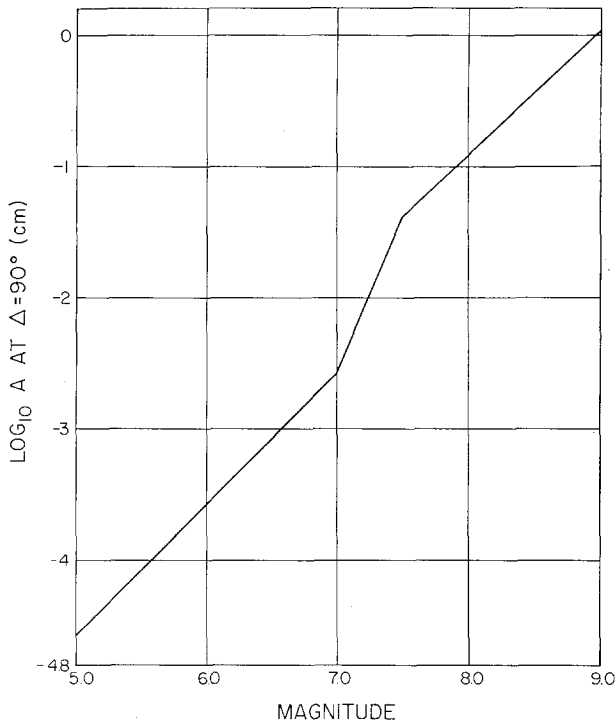


FIG. 4. Logarithm to the base 10 of the amplitude of vertical ground motion (in cms.) of 100 second period mantle Rayleigh waves at a distance of 90° , plotted as a function of magnitude M (Brune and King, 1967). This curve is used in the definition of mantle wave magnitude.

and in Figure 4 for Rayleigh waves. The distance correction curve for Rayleigh waves is given in Figure 5 (combining the two correction curves given by Brune and King, 1967). Note that for Rayleigh waves, ground amplitude is used, and for Love waves ground spectral density is used. Ground amplitude may be approximately converted to spectral density for the Love waves by multiplying by 70 seconds. This approximation will be best if the G-wave pulse has a predominant period of about 100 seconds and will not be valid if the predominant period varies greatly from this; Fourier analysis should be used. The approximation has not been used in this study but can

be used for preliminary assignment of mantle-wave magnitude. The instruments described by Gilman (1960) are ideal for using this definition of magnitude, since their peak response is near 100 seconds.

A 3-component, long-period, low magnification seismograph system specially designed to record mantle waves has recently been installed at Cal-Tech. The system uses 35-second pendulums with electromagnetic transducers, coupled to 100-second galvanometers through a 2-stage low-pass filter. This arrangement yields a period-magnification response peaking at 100 seconds with maximum magnification of 25. Low sensitivity is used with the hope of obtaining on scale recordings of low order

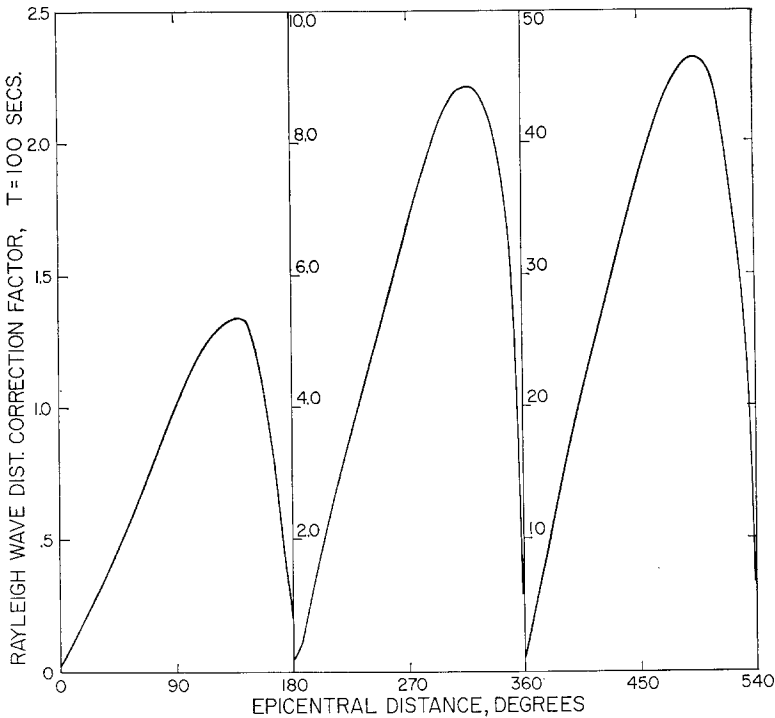


FIG. 5. Amplitude distance correction factor for 100 second period mantle Rayleigh waves (combining factors *A* and *B* of Brune and King, 1967).

mantle waves from the largest teleseisms. However, even with the low sensitivity mantle waves are clearly recorded from shocks as small as $M = 6.0$.

Using the mantle wave magnitude scale, we have determined mantle wave magnitudes M_M for several of the largest earthquakes since 1930, and these results are presented in Table 4. The largest earthquake of those examined since 1930 based on this scale is the Alaskan earthquake of March 28, 1964 ($M_M = 8.9$); other earthquakes of comparably large size ($M_M = 8.8$) are the Kamchatka earthquake of November 4, 1952 and the Chilean earthquake of May 22, 1960. Surprisingly the Sanriku, Japan, earthquake of March 2, 1933 which is given a magnitude of 8.9 by Gutenberg (1956) has a mantle wave magnitude of only 8.4. Thus the very long-period excitation by this earthquake was relatively small.

MANTLE WAVES AS A DIAGNOSTIC AID FOR THE TSUNAMI WARNING SYSTEM

Since Seismic Sea waves are very long period it might be expected that the mantle wave magnitude of an earthquake would be a more suitable diagnostic aid for Tsunami

warnings than the ordinary 20 second surface wave magnitude. The critical earthquake for testing this idea is the April 1st, 1946 Aleutian earthquake which caused a destructive Tsunami even though the surface wave magnitude was only 7.4. The mantle wave magnitude for this event, determined by averaging 11 phases at 8 stations is 7.8. Thus the long-period excitation was relatively great and using the mantle wave magnitude we would have considered this earthquake more likely to generate a Tsunami than we would have using the 20 second surface wave magnitude. This suggests that whenever possible the mantle wave magnitude should be used as a diagnostic aid in estimating the Tsunami potential of an earthquake.

TABLE 4
MANTLE WAVE MAGNITUDES

No.	Date	Location of Earthquake	Pas Mag	Mantle Wave Mag	# of Stations Read	% of Phases Averaged
1	3/28/64	Alaska	8.4	8.9	4	8
2	11/4/52	Kamchatka	8.4	8.8	7	17
3	5/22/60	Chile	8 $\frac{1}{4}$ -8 $\frac{1}{2}$	8.8	3	5
4	8/15/50	Assam	8.7	8.7	2	3
5	2/3/23	Kamchatka	8.4	8.7†	1	4
6	8/10/31	Mongolia	7.9	8.6†	1	2
7	2/1/38	New Guinea	8.6	8.5	3	7
8	6/17/28	Mexico	7.9	8.4†	1	3
9	3/2/33	Sanriku	8.9	8.4	4	6
10	11/10/38	Alaska Peninsula	8.7	8.3	2	4
11	3/4/52	Japan	8.6	8.3	3	7
12	6/3/32	Mexico	8.1	8.2	2	4
13	9/1/23	Tokyo	8.3	8.2†	1	2
14	5/24/40	Peru	8.4	8.1*	2	3
15	1/15/34	India	8.4	8.0	2	3
16	6/26/41	Andaman Isls.	8.7	8.0*	2	5
17	5/14/32	Halmahera Isls.	8.3	7.9	3	7
18	12/1/28	Chile	8.3	7.9†	1	2
19	8/24/42	Peru	8.6	7.9*	2	5
20	8/6/42	Guatemala	8.3	7.9*	2	4
21	7/18/34	Santa Cruz Isls.	8.1	7.8†	1	3

* $H = 50-60$ km.

† Magnitude based on one station may not be representative.

CONCLUSIONS

(1) A curve for the excitation of 100-second period mantle Love waves as a function of Pasadena magnitude has been obtained from 153 measurements of spectral density of mantle Love waves.

(2) The curve for excitation of mantle Love waves as a function of magnitude agrees with the curve for excitation of mantle Rayleigh waves of 100-second period obtained by Brune and King (1967), and, in the case of strike-slip motion, agrees with the curve for seismic moment versus magnitude obtained by Brune (1968). For dip-slip motion, the curve for seismic moment should be multiplied by a factor of about $2\frac{1}{2}$.

(3) A definition of mantle-wave magnitude has been set up, and the largest earthquake since 1930 found on this scale is the Alaskan earthquake of March 28, 1964; $M_M = 8.9$. Other comparably large earthquakes, $M_M = 8.8$, were the Kamchatka earthquake of November 4, 1952 and the Chilean earthquake of May 22, 1960.

(4) It is suggested that mantle wave magnitude be used as a diagnostic aid in estimating the Tsunami potential of an earthquake. The Aleutian earthquake of April 1, 1946 is given as an example of an earthquake which generated a destructive Tsunami and for which the mantle wave magnitude (7.8) would have been more indicative of Tsunami potential than the surface wave magnitude (7.4).

ACKNOWLEDGMENTS

The authors are indebted to Professor Charles F. Richter for critically reading the manuscript and offering constructive criticism. Thanks are due Mr. Ralph Gilman who provided records and calibration curves from the Pasadena (PAS) ULP instruments, and to the U. S. Coast and Geodetic Survey for supplying records. This research was supported by the National Science Foundation under Grant GA 1087 (Earthquake Mechanism).

REFERENCES

- Ben-Menahem, A. (1965). Observed attenuation and Q values of seismic surface waves in the Upper Mantle, *J. Geophys. Res.* **70**, 4641-4651.
- Ben-Menahem, A. and D. G. Harkrider (1964). Radiation patterns of seismic surface waves from buried dipolar point sources in a flat stratified Earth, *J. Geophys. Res.* **69**, 2605-2620.
- Brune, J. N. (1968). Seismic moment, seismicity, and rate of slip along major fault zones, *J. Geophys. Res.* **73**, 777-784.
- Brune, J. N. and C. R. Allen (1967). A low-stress-drop, low magnitude earthquake with surface faulting: the Imperial, California earthquake of March 4, 1966, *Bull. Seism. Soc. Am.* **57**, 501-514.
- Brune, J. N. and C. Y. King (1967). Excitation of mantle Rayleigh waves of period 100 seconds as a function of magnitude, *Bull. Seism. Soc. Am.* **57**, 1355-1365.
- Byerly, P. (1926). The Montana earthquake of June 28, 1925, G.M.C.T., *Bull. Seism. Soc. Am.* **16**, 209-265.
- Gilman, R. (1960). Report on some experimental long-period seismographs, *Bull. Seismo. Soc. Am.* **50**, 553-559.
- Gutenberg, B. (1956). Great earthquakes 1896-1903, *Trans. Am. Geophys. U.* **37**, 608-614.
- Gutenberg, B. and C. F. Richter (1954). *Seismicity of the Earth and Associated Phenomena*, New York, Hafner Publishing Co., 310 p.
- Maruyama, T. (1963). On the force equivalents of dynamical elastic dislocations with reference to the earthquake mechanism, *Bull. of Earthquake Res. Inst.* **41**, 467-486.
- Richter, C. F. (1958). *Elementary Seismology*, San Francisco, W. H. Freeman and Co., 768 p.

SEISMOLOGICAL LABORATORY
CALIFORNIA INSTITUTE OF TECHNOLOGY
PASADENA, CALIFORNIA
DIVISION OF GEOLOGICAL SCIENCES
CONTRIBUTION No. 1559

Manuscript received September 16, 1968.